SCI INSTITUTE

TECHNICAL REPORT

Implementation and Verification of a Nodally-Integrated Tetrahedral Element in FEBio

Steve A. Maas, Benjamin J. Ellis, David S. Rawlins, Lowell T. Edgar, Corinne R. Henak and Jeffrey A. Weiss

UUSCI-2011-007

Scientific Computing and Imaging Institute
University of Utah
Salt Lake City, UT 84112 USA

December 28, 2011

Abstract:

Finite element simulations in computational biomechanics commonly require the discretization of extremely complicated geometries. Creating meshes for these complex geometries can be very difficult and time consuming using hexahedral elements. Automatic meshing algorithms exist for tetrahedral elements, but these elements often have numerical problems that discourage their use in complex finite element models. To overcome these problems we have implemented a stabilized, nodally-integrated tetrahedral element formulation in FEBio, our in-house developed finite element code, allowing researchers to use linear tetrahedral elements in their models and still obtain accurate solutions. In addition to facilitating automatic mesh generation, this also allows researchers to use mesh refinement algorithms which are fairly well developed for tetrahedral elements but not so much for hexahedral elements. In this document, the implementation of the stabilized, nodally-integrated, tetrahedral element, named the “UT4 element”, is described. Two slightly different variations of the nodally integrated tetrahedral element are considered. In one variation the entire virtual work is stabilized and in the other one the stabilization is only applied to the isochoric part of the virtual work. The implementation of both formulations has been verified and the convergence behavior illustrated using the patch test and three verification problems. Also, a model from our laboratory with very complex geometry is discretized and analyzed using the UT4 element to show its utility for a problem from the biomechanics literature. The convergence behavior of the UT4 element does vary depending on problem, tetrahedral mesh structure and choice of formulation parameters, but the results from the verification problems should assure analysts that a converged solution using the UT4 element can be obtained that is more accurate than the solution from a classical linear tetrahedral formulation.

THE UNIVERSITY OF UTAH

1 Introduction

Simulations in computational biomechanics commonly require the segmentation and finite element (FE) discretization of extremely complicated geometries. Medical image data is by far the most common source of 3D geometric information for segmentation and mesh generation. However, mesh generation can be very difficult and time consuming due to complex geometry (Figure 1).

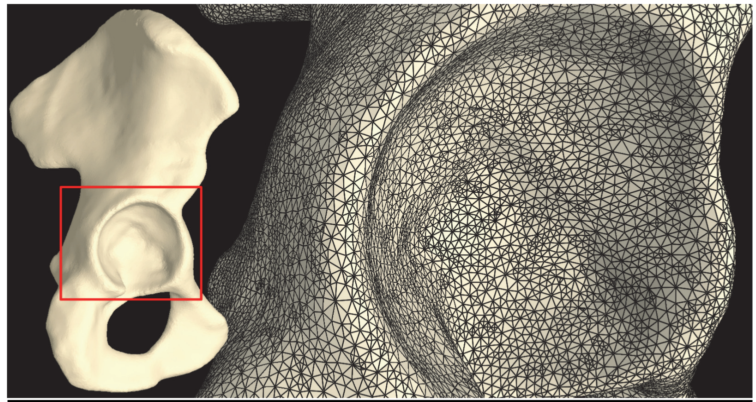

Figure 1: Example of an unstructured tetrahedral mesh for a human hemipelvis. Tetrahedral elements were generated using an unstructured tetrahedral mesh generator to represent cortical pelvic bone.

Robust automatic mesh generation algorithms exist for triangular and tetrahedral meshes such as Delaunay triangulation [1, 2], advancing front [3-5] or octree techniques [6]. Triangular and tetrahedral elements can be very effective for FE analyses of field variables on non-deforming meshes, such as for electrodynamics and fluid mechanics, and tetrahedral meshes facilitate the use of adaptive mesh refinement techniques [7-10]. However, when used in large deformation solid mechanics, linear tetrahedral elements are overly stiff and can "lock" in problems where nearly incompressible materials and/or acute bending are encountered [11]. Although the locking can be alleviated by the use of higher-order (e.g., quadratic) tetrahedral elements, they are more computationally demanding and are more prone to Jacobian inversions during nonlinear Newton or quasi-Newton iterations.

Because of these issues, trilinear hexahedral elements are often preferred to tetrahedral elements in nonlinear solid mechanics. Although serveral algorithms for automatic hexahedral mesh generation have been reported [12][13], the approaches are not always robust and for this reason they have not been widely used. Thus, analysts in the field of computational biomechanics are often forced to generate hexahedral meshes using semi-automatic mapping algorithms, which require a considerable amount of time and effort. The limitations of mapped meshing techniques using hexahedral elements are especially problematic when the analyst wishes to generate multiple meshes, as is the case for patient- or subject-specific modeling.

The simplicity of tetrahedral meshing schemes motivates the need for a robust, linear tetrahedral element formulation that behaves well in problems involving nearly incompressible materials and bending deformations. Such an element would allow analysts to take advantage of automatic mesh generation and adaptive refinement available with tetrahedral meshes without the inaccuracies inherent to the linear tetrahedral element. Improving the behavior of linear tetrahedral elements is currently the topic of considerable research effort within the field of computational solid mechanics. Recent reports in the literature describe tetrahedral finite elements that circumvent problems associated with classic tetrahedral elements by using enhanced strain fields or additional degrees of freedom, such as pressure and volume ratio in addition to nodal displacements [14-16]. For example, the implementation of "composite tetrahedral elements" can eliminate volumetric locking for nearly incompressible problems [14-16]. The linear tetrahedral element with nodal interpolated pressures and bubble modes developed by Taylor circumvents problems associated with incompressible material behavior, but requires pressure as an additional degree of freedom and is not efficient when representing bending deformations [16]. An alternative approach is the averaged nodal deformation gradient linear tetrahedral element, also known as the nodally-integrated tetrahedral element. Different forms of this element have been investigated by Bonet et al. [17] and Dohrmann et al. [15]. The strain averaging that is necessary to efficiently capture bending can cause instabilities. Elements without average shear strains avoid the instabilities, but lock in bending. With the exception of this shortcoming, these new formulations have proven to be very effective.

The ten node tetrahedral element with piecewise discontinuous linear pressure/volume interpolations and bubble modes is another potential option. This element satisfies the LBB criterion [11, 18], provides second order convergence in the energy norm even in the presence of incompressibility and is suitable for bending. On the other hand, the element is considerably more susceptible to element inversions than lower-order elements due to the quadratic shape functions, is currently not suitable for contact analyses and may not have a diagonalizable mass matrix.

The method proposed by Dohrmann et al. [15] is particularly attractive since it works well for both bending and incompressibility and provides good convergence behavior. Although the authors mentioned that spurious low frequencies could be detected in eigenvalue calculations, the investigators had no difficulties with instabilities. Nonetheless, Puso et al. identified a spurious mode and formulated a stabilization technique [19]. The stabilization technique is simple and, unlike the SUPG stabilization recommended in [17], preserves symmetry in the stiffness matrix.

The formulation introduced by Puso et al. attempts to resolve the instabilities inherent in nodally-integrated tetrahedral formulations by adding the virtual work that corresponds to the classical linear tetrahedral formulation to the total virtual work, multiplied by a user-controlled scaling factor. Although this may stabilize the formulation, this also re-introduces locking unless the second term uses a different "softer" constitutive model. Gee et al. avoids this problem, by applying the stabilization only to the isochoric part of the stress [20]. The Gee et al. version of the stabilized, nodally-integrated, tetrahedral element has been implemented in FEBio. This will encourage the use of automatic mesh generation, mesh refinement, and analysis of models that are very difficult to discretize using hexahedral elements.

Finally, both Gee et al. [20] and Dohrmann et al. [15] refer to their formulations as the Uniform Nodal Strain 4-node tetrahedral element, or "UT4 element", and this acronym is maintained in the FEBio implementation and documentation, as well as in this document.

2 Theory and Implementation

The nodally-integrated tetrahedral element that is implemented in FEBio follows Gee's formulation [20] closely. Like the classical linear tetrahedral element, this formulation is a displacement-only formulation using linear shape functions, but applies nodal averaging to the deformation gradient to prevent element locking. A nodally averaged deformation gradient $\mathbf{F}^I$ at node I is defined as,

$$\mathbf{F}^I = \frac{1}{V^I} \sum_{e \in S_I^{el}} \frac{V^e}{4} \mathbf{F}^e , \tag{1.1}$$

where S_I^{el} is the patch of elements adjacent to node I, V^e is the volume of element e, $\mathbf{F}^e$ is the deformation gradient of element e, and $V^I = \frac{1}{4} \sum_{e \in S_I^{el}} V^e$ is the nodally averaged volume of node I.

The internal part of the weak form of the governing equations is now written as a sum of a nodal and an element-wise contribution:

$$\delta W^{\text{int}} = \delta W_{nd}^{\text{int}} + \delta W_{el}^{\text{int}} = \sum_I V^I \delta \mathbf{E}^I : (1-\alpha) \mathbf{S}^I + \sum_e \int_{\Omega^e} \delta \mathbf{E}^e : \alpha \mathbf{S}^e d\Omega^e . \tag{1.2}$$

The parameter $0 < \alpha < 1$ is a stabilization parameter, assumed to be constant throughout the domain, and $\mathbf{E}^I$ are nodally averaged Green-Lagrange strains obtained from (1.1). The stresses $\mathbf{S}^I$ and $\mathbf{S}^e$ are the nodally averaged and element stresses, respectively.

Choosing $\alpha = 0$ corresponds to the unstabilized nodal strain approach, which is known to be unstable. The choice $\alpha > 0$ is essentially the formulation proposed by Puso, except the same material law is used in both terms. As mentioned above, this may re-introduce locking. Gee proposed applying the stabilization only to the isochoric part of the internal work. In his formulation, the internal part of the virtual work takes on the following form:

$$\delta W^{\text{int}} = \sum_I V^I \delta\mathbf{E}^I : \left(\mathbf{S}^I - \alpha\mathbf{S}^I_{\text{iso}}\right) + \sum_e \int_{\Omega^e} \delta\mathbf{E}^e : \alpha\mathbf{S}^e_{\text{iso}} d\Omega^e \, , \tag{1.3}$$

where the stress is split into volumetric and isochoric terms, $\mathbf{S} = \mathbf{S}_{vol} + \mathbf{S}_{\text{iso}}$.

Both formulations (equation (1.2) and (1.3)) have been implemented in FEBio. The user can choose between the two by requesting the desired formulation in the input file. In the rest of the document we refer to the formulation in equation (1.2) as the *Iso0* formulation, whereas equation (1.3) will be referred to as the *Iso1* formulation. The user can also set the value for the stabilization parameter α in the input file. The recommended range for this parameter is 0.05 < α < 0.2, consistent with the studies by Gee [20] and Puso [19], as well as with our own findings below.

3 Verification Problems

Four problems were used to verify the performance of the UT4 element implemented in FEBio. Results from models using the UT4 formulation were compared to an analytical solution or to a numerical solution when available, or to the converged solution of a three-field hexahedral element mesh [21, 22]. Both the formulation that stabilizes the entire internal work (Iso0) and the formulation that only stabilizes the isochoric part of the internal work (Iso1) were investigated. Additionally, both the Iso0 and Iso1 formulations were used with α parameter values of 0.05, 0.1, and 0.2. This yielded six parameter combinations per problem, and each set of parameters were used with three mesh densities for problems 3.2, 3.3, and 3.4. Both structured and unstructured meshes were used for problem 3.3. to show the effects of these mesh types. Finally, the last problem uses the UT4 element to discretize a model from our laboratory with very complex geometry. The parameter combinations and meshes for problems 3.2, 3.3, and 3.4 that most closely matched the numerical or hexahedral element solutions have been added to the FEBio test suite (http://mrl.sci.utah.edu/software/febio).

3.1 Patch Test

The 3D patch test proposed by MacNeal & Harder [23] was used to verify the implementation of the UT4 element formulation in FEBio (Figure 2). The positions of the interior nodes are listed in Table 1. The exterior nodes were assigned a displacement at time t = 1.0 according to the formulas provided in Table 2. A linear elastic material is used with coefficients $E = 10^6$ psi and $v = 0.25$.

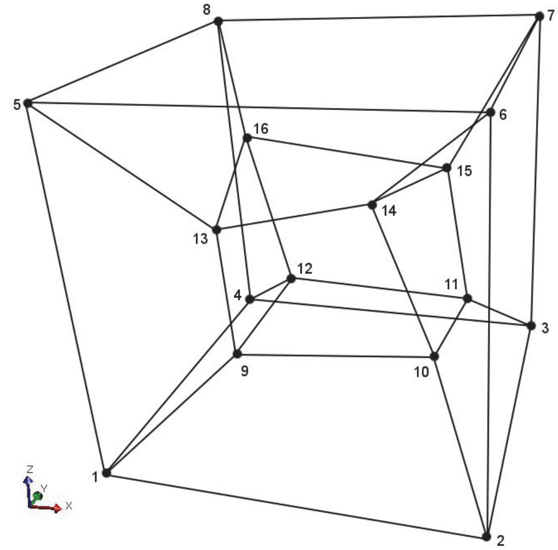

Figure 2: Patch test geometry. Unit cube with node 1 located at the origin.

Nodes	x	y	z
9	0.249	0.342	0.192
10	0.826	0.288	0.288
11	0.850	0.649	0.263
12	0.273	0.750	0.230
13	0.320	0.186	0.643
14	0.677	0.305	0.683
15	0.788	0.693	0.644
16	0.165	0.745	0.702

Table 1: Interior node coordinates

u	$10^{-3}(2x + y + z)/2$
v	$10^{-3}(x + 2y + z)/2$
w	$10^{-3}(x + y + 2z)/2$

Table 2: Displacement at time t = 1.

The analytical solution provided by MacNeal & Harder was $\sigma_x = \sigma_y = \sigma_z$ = 2000 psi and $\sigma_{xy} = \sigma_{yz} = \sigma_{zx}$ = 400 psi [23]. The UT4 mesh resulted in homogeneous stresses with the values given by the analytical solution, and therefore passed the patch test for all cases considered.

3.2 Bending Beam Problem

A nearly-incompressible bending beam was analyzed to examine the shear locking behavior of the UT4 element (Figure 3). The beam measured 2 × 2 × 16 and was represented by an uncoupled hyperelastic neo-Hookean constitutive model ($C_1 = 6.667 \times 10^6$, $K = 5.0 \times 10^9$) [20]. Shear traction of 2000 was applied to one end of the beam while the other end was rigidly fixed. The maximum tip displacement was obtained from each analysis and compared against the analytical solution (Figure 4).

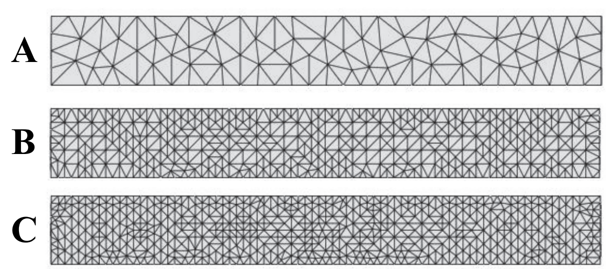

Figure 3: Unstructured tetrahedral meshes for bending beam problem. (A) 1406 elements, (B) 12497 elements, (C) 24749 elements.

Beams discretized with UT4 Iso0 elements softened (that is, produced larger tip displacements) with increased mesh density, as would be expected. In contrast, beams stiffened when using the UT4 Iso1 formulation, resulting in smaller tip displacements with increased mesh density. For the Iso0 formulation, tip displacements decreased as α increased for each mesh density. In contrast, for the Iso1 formulation tip displacements increased slightly as α increased for each mesh density, but these increases were relatively small for the two larger mesh densities. The UT4 element did not experience shear locking with the combinations of parameters and mesh densities used for this problem. The resulting tip displacement of the beam with the densest tetrahedral mesh using the Iso1 formulation and a stabilization parameter value of α = 0.2 was nearly identical to the previously published numerical solution [24].

3.3 Cook's Membrane Problem

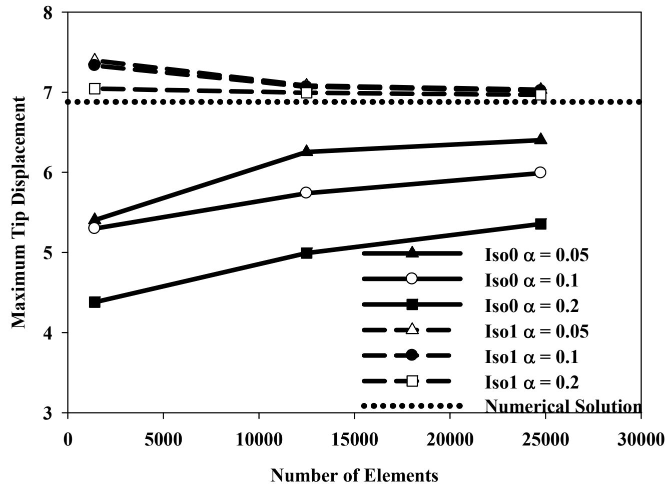

Figure 4: Convergence behavior of the UT4 element with and without isochoric stabilization and with α values of 0.05, 0.1, and 0.2. UT4 predictions approached the numerical solution from below without isochoric stabilization (iso0), and from above with isochoric stabilization (iso1).

Cook's membrane problem was used to test the combined bending and shearing response of the UT4 element. The tapered panel used in the problem measured 44 mm at the left vertical edge, 16 mm at the right vertical edge, and these two parallel edges were 48 mm apart (Figure 5). The depth of the panel was 1 mm in the z direction. The panel was composed of an uncoupled neo-Hookean material (C_1 = 40.1 KPa, K = 40094 KPa). The left edge of the panel was fixed to prevent motion in the x and y directions, and a traction force of 50 KPa was applied in the y direction to the right face of the panel. The problem was analyzed under plane strain boundary conditions by preventing motion in the z direction. The y-component of the displacement vector measured at the upper-right corner of the panel was recorded for all simulations as a measure of combined bending and shearing response.

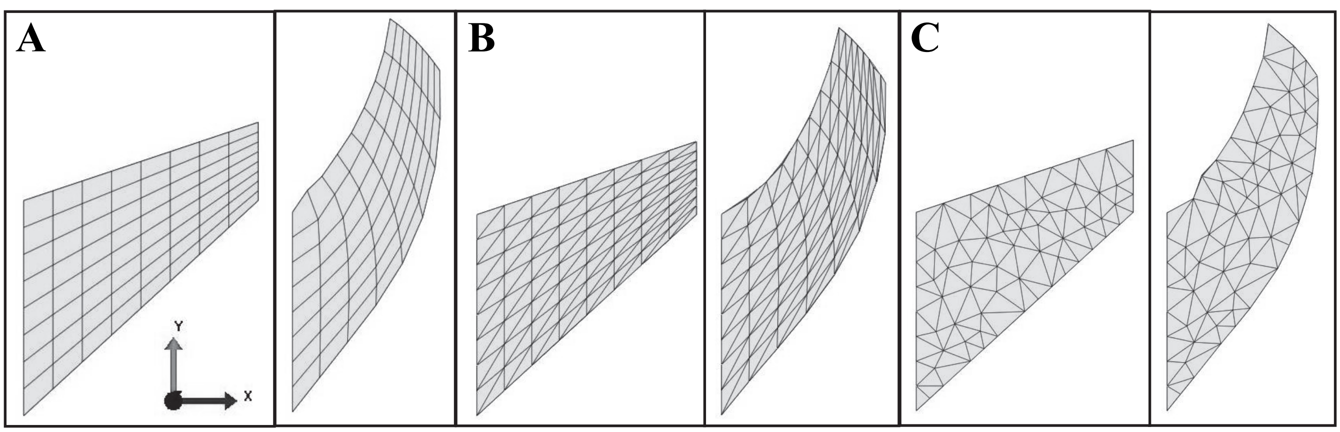

Figure 5: Cook's Membrane problem. (A) Three-field hexahedral mesh (64 elements), initial geometry on the left and deformed geometry on the right. (B) Structured UT4 mesh (404 elements). (C) Unstructured UT4 mesh (345 elements).

The Cooke's membrane was analyzed using structured and unstructured meshes with a single-element through the thickness. Structured UT4 meshes had the following resolution levels: 404, 7041, 24576 elements, while the unstructured UT4 meshes had: 345, 6955, 22557 elements. Each structured and unstructured UT4 mesh was analyzed using the Iso0 or Iso1 formulation with parameters α = 0.05, 0.1, and 0.2. The bending and shearing response of all UT4 meshes was compared to the solution of a converged hexahedral mesh, which produced a displacement of 27.4 mm (Figure 6).

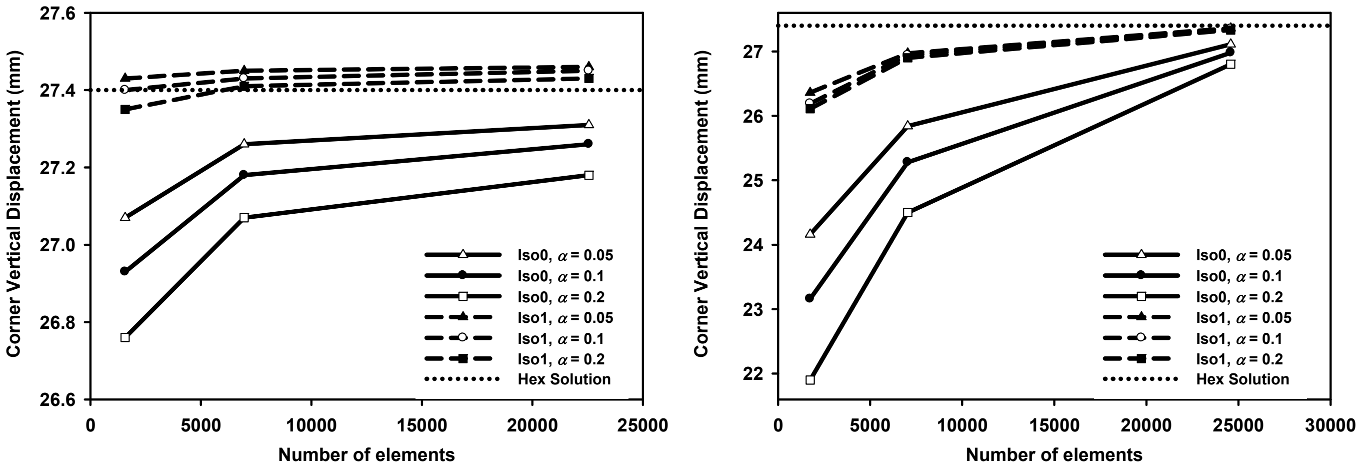

Figure 6: Convergence behavior of the UT4 element for Cook's membrane problem. Left) Structured UT4 mesh results. Right) Unstructured mesh results. Structured UT4 meshes required fewer elements to match the converged hexahedral result than the unstructured UT4 meshes. Models using the Iso1 formulation performed much better than models using the Iso0 formulation.

In general, structured UT4 meshes were better at matching the converged hexahedral result than the unstructured UT4 meshes. For the Cooke's membrane problem, models using both the Iso0 and Iso1 formulations softened, producing larger corner vertical displacements, with increased mesh density, as would be expected. For both structured and unstructured meshes, models using the Iso1 formulation were able to match the hex solution with fewer elements than the models using the Iso0 formulation. Further, for both structured and unstructured meshes, using either Iso0 or Iso1 formulation, the model softened as the α parameter was decreased. In conclusion, for the Iso1 formulation, there was a mesh density for both structured and unstructured meshes for which the solution was nearly identical to the converged hex solution. However, the structured meshes required far fewer elements.

3.4 Twisted Cylinder Problem

A hollow cylinder (inner diameter 1, outer diameter 2, height 1) was subjected to twist about the long axis by applying equal and opposite rigid body rotations of 0.4 radians to the inner and outer surfaces (Figure 7). To eliminate rigid-body modes, a ring of nodes on one flat face at a radius of 1.5 was constrained in all 3 translational degrees of freedom. A plane-stress condition was defined for the opposite flat face. This problem tests the convergence behavior of the UT4 element when subjected to shear loading and used with a nearly-incompressible material. For this problem an uncoupled neo-Hookean constitutive equation (C_1 = 10, K = 10,000) was used to represent the cylinder material. Three structured tetrahedral meshes with increasing density were analyzed. As with the previous problems, the model was analyzed with and without isochoric stabilization and using three alpha values (0.05, 0.1, and 0.2). Results for the UT4 models were compared to the solution from a converged three-field hexahedral mesh.

The results for this problem were similar to the bending beam problem. Models using the Iso1 formulation produced results that were softer than the converged hexahedral solution and models using the Iso0 formulation produced results that were stiffer (Figure 7). Unlike the bending beam problem, increasing the number of elements softened the model results for either stabilization parameter. Finally, increasing α produced stiffer model results for both formulations.

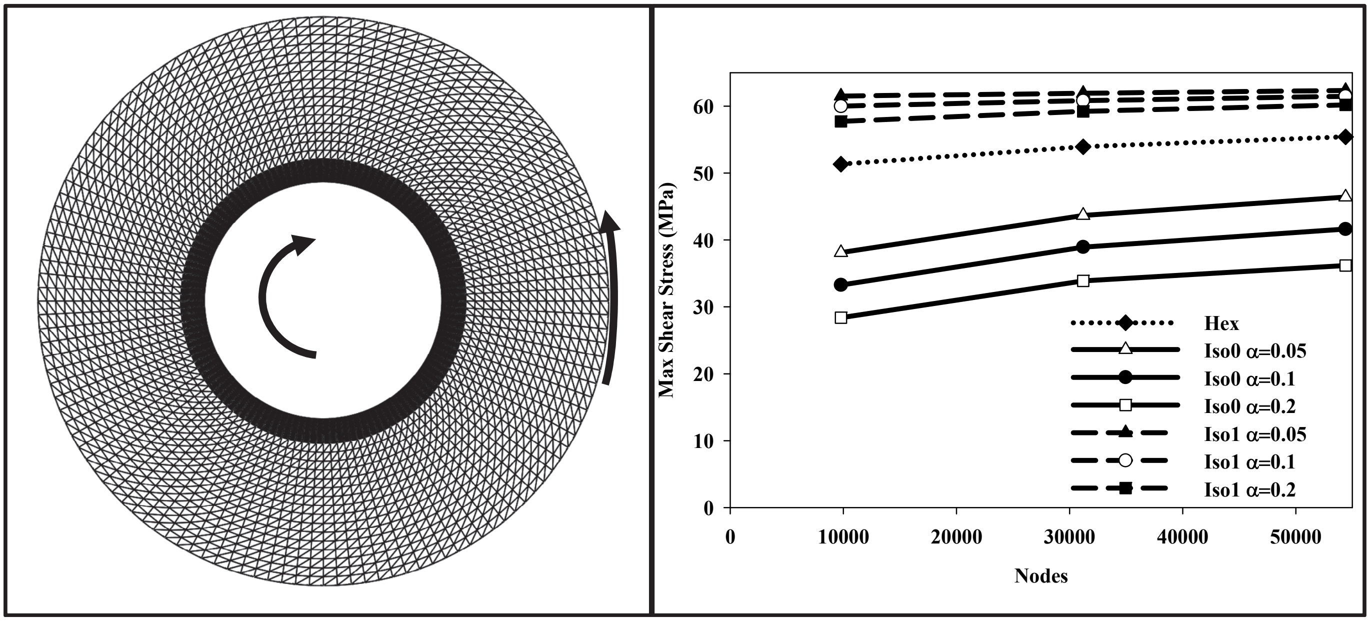

Figure 7: Left) Hollow cylinder discretized with a structured tetrahedral mesh. Arrows indicate directions of 0.4 radian rotations applied to inner and outer surfaces. Right) Graph of maximum shear stress at the inner surface of the cylinder showing the convergence behavior of the UT4 element with Iso0 and Iso1 formulations, as well as with α = 0.05, 0.1, and 0.2.

3.5 Example from Biomechanics Literature

To illustrate the utility of the UT4 element, a model from our previously published research was discretized and analyzed using the UT4 element formulation [25]. The model represents the helical fibril organization within the crimped fiber of ligament or tendon (Figure 8). The complex geometry of this model was particularly difficult to mesh with hexahedral elements, making it a good problem for considering tetrahedral element discretization. The boundary and loading conditions for this problem were also quite complex. The model shown in Figure 8 was the periodic unit cell in a computational homogenization problem using periodic boundary conditions [25]. A neo-Hookean constitutive model was used to represent both the fibril and matrix materials. The fibril shear modulus was two orders of magnitude larger than the matrix modulus, giving rise to the distinct difference in stresses. The model geometry, a helical fibril organization within a crimped fiber, was capable of simultaneously predicting the large Poisson's ratios and the nonlinear stress–strain behavior observed when testing ligament and tendon.

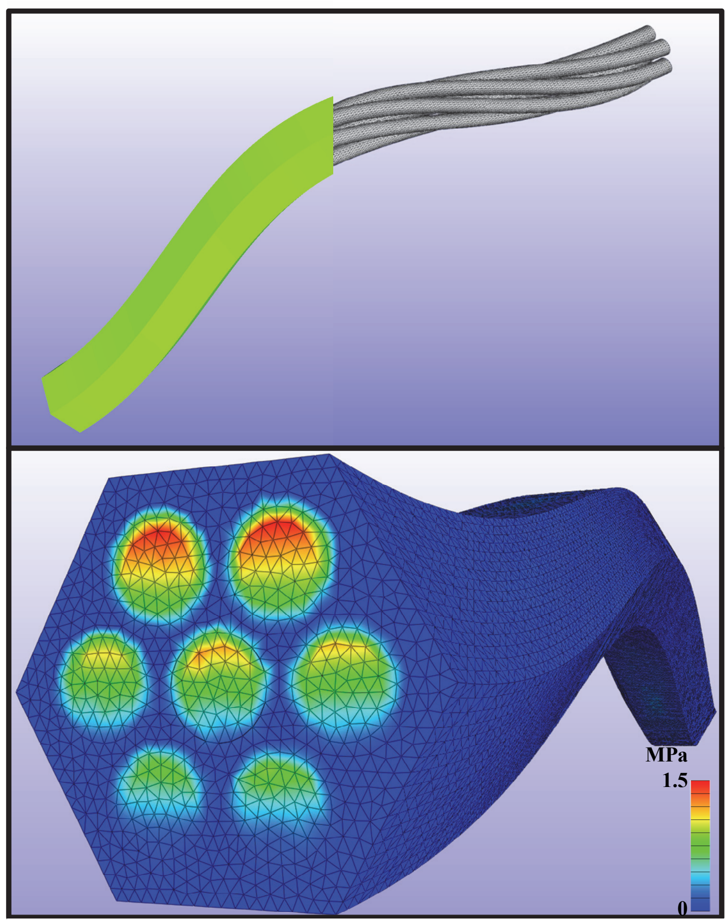

Figure 8. Top) Model of helical fibrils within a crimped fiber. Bottom) Predicted effective stress caused by an applied tension.

4 Conclusions

Due to the varying convergence behavior of the UT4 element depending on problem, tetrahedral mesh structure, choice of Iso0 or Iso1 formulation and α parameter, it is strongly advised that analysts conduct a thorough mesh verification for their particular problem. The time to conduct this mesh verification using the UT4 element will need to be weighed against the time to mesh and verify the mesh using hexahedral elements. In the end, the results from these verification problems should assure analysts that a converged solution using the UT4 element can be obtained. Also, the Cooke's membrane and twisted cylinder problems show that analysts can often use relatively fewer tetrahedral elements when using the UT4 formulation.

In conclusion, the UT4 element in FEBio allows researchers to use linear tetrahedral elements in models where the numerical problems inherent to the classical linear tetrahedral element would have been prohibitive, or would have required the use of hexahedral element formulations that are more time consuming in terms of mesh generation. In all problems considered above, the new UT4 formulation was able to find a more accurate solution than the classical tetrahedral element, illustrating its superior behavior.

5 Acknowledgments

Financial support from NIH #R01GM083925 is gratefully acknowledged. The authors thank Dr. Michael Puso of Lawrence Livermore National Laboratory for his assistance with implementation and debugging of the UT4 element.

6 References

1. Delaunay, B.N.S.l.S.V.I.A.N.S., VII Seria, Otdelenie Matematicheskii i Estestvennyka Nauk Vol 7 pp.793-800, *"Sur la Sphere" Vide.* Izvestia Akademia Nauk SSSR, VII Seria, Otdelenie Matematicheskii i Estestvennyka Nauk, 1934. **7**: p. 793-800.
2. Wrazidlo, W., et al., *An alternative method of three-dimensional reconstruction from two-dimensional CT and MR data sets.* Eur J Radiol, 1991. **12**(1): p. 11-6.
3. Lo, S.H., *Volume Discretization into Tetrahedra-I. Verification and Orientation of Boundary Surfaces.* Computers and Structures, 1991. **39**(5): p. 493-500.
4. Lo, S.H., *Volume Discretization into Tetrahedra - II. 3D Triangulation by Advancing Front Approach.* Computers and Structures, 1991. **39**(5): p. 501-511.
5. Lohner, R., *Progress in Grid Generation via the Advancing Front Technique.* Engineering with Computers, 1996. **12**: p. 186-210.
6. Shephard, M.S. and M.K. Georges, *Three-Dimensional Mesh Generation by Finite Octree Technique.* International Journal for Numerical Methods in Engineering, 1991. **32**: p. 709-749.
7. Hubsch, P.F., et al., *Adaptive finite-element approach for analysis of bone/prosthesis interaction.* Med Biol Eng Comput, 1995. **33**(1): p. 33-7.
8. Johnson, C.R. and R.S. MacLeod, *Adaptive local regularization methods for the inverse ECG problem.* Prog Biophys Mol Biol, 1998. **69**(2-3): p. 405-23.

9. Prakash, S. and C.R. Ethier, *Requirements for mesh resolution in 3D computational hemodynamics.* J Biomech Eng, 2001. **123**(2): p. 134-44.
10. Spilker, R.L., E.S. de Almeida, and P.S. Donzelli, *Finite element methods for the biomechanics of soft hydrated tissues: nonlinear analysis and adaptive control of meshes.* Crit Rev Biomed Eng, 1992. **20**(3-4): p. 279-313.
11. Zienkiewicz, O.C. and R.L. Taylor, *The Finite Element Method, Volume 1: Basic Formulation and Linear Problems*. 1989, London.
12. Blacker, T.D. and R.J. Meyers, *Seams and wedges in plastering: A 3-D hexahedral mesh generation algorithm.* Engineering with Computers (New York), 1993. **9**(2): p. 83-93.
13. Tautges, T.J., T. Blacker, and S.A. Mitchell, *Whisker weaving algorithm: A connectivity-based method for constructing all-hexahedral finite element meshes.* International Journal for Numerical Methods in Engineering, 1996. **39**(19
Oct 15): p. 3327-3349.
14. Beissel, S.R. and G.R. Johnson, *Large-deformation triangular and tetrahedral element formulations for unstructured meshes.* Computer Methods in Applied Mechanics and Engineering, 2000. **187**(3
Jul): p. 469-482.
15. Dohrmann, C.R., et al., *Node-based uniform strain elements for three-node triangular and four-node tetrahedral meshes.* International Journal for Numerical Methods in Engineering, 2000. **47**(9): p. 1549-1568.
16. Taylor, R.L., *Mixed-enhanced formulation for tetrahedral finite elements.* International Journal for Numerical Methods in Engineering, 2000. **47**(1
Jan): p. 205-227.
17. Bonet, J., H. Marriott, and O. Hassan, *An averaged nodal deformation gradient linear tetrahedral element for large strain explicit dynamic applications.* Communications in Numerical Methods in Engineering, 2001. **17**(8
August): p. 551-561.
18. Bathe, K.-J., *Finite Element Procedures in Engineering Analysis.* 1982.
19. Puso, M.A. and J. Solberg, *A stabilized nodally integrated tetrahedral.* International Journal for Numerical Methods in Engineering, 2006. **67**(6): p. 841-867.
20. Gee, M.W., et al., *A uniform nodal strain tetrahedron with isochoric stabilization.* International Journal for Numerical Methods in Engineering, 2009. **78**(4): p. 429-443.
21. Simo, J.C. and R.L. Taylor, *Quasi-incompressible finite elasticity in principal stretches: Continuum basis and numerical algorithms.* Computer Methods in Applied Mechanics and Engineering, 1991. **85**: p. 273-310.
22. Weiss, J.A., B.N. Maker, and S. Govindjee, *Finite element implementation of incompressible, transversely isotropic hyperelasticity.* Computer Methods in Applications of Mechanics and Engineering, 1996. **135**: p. 107-128.
23. MacNeal, R.H. and R.L. Harder, *A proposed set of problems to test finite element accuracy.* Finite Elements in Analysis and Design, 1985. **1**(1): p. 3-20.
24. Belendez, T., C. Neipp, and A. Belendex, *Large and small deflections of a cantilever beam*, in *European Journal of Physics*. 2002. p. 371.
25. Reese, S.P., S.A. Maas, and J.A. Weiss, *Micromechanical models of helical superstructures in ligament and tendon fibers predict large Poisson's ratios.* Journal of biomechanics, 2010. **43**(7): p. 1394-400.